Special Issue

Optical Coherence Tomography Angiography

Simon S. Gao, Yali Jia, Miao Zhang, Johnny P. Su, Gangjun Liu, Thomas S. Hwang, Steven T. Bailey, and David Huang

Casey Eye Institute, Oregon Health & Science University, Portland, Oregon, United States

Correspondence: David Huang, Casey Eye Institute, Oregon Health & Science University, 3375 S.W. Terwilliger Boulevard, Portland, Oregon 97239, USA; davidhuang@alum.mit.edu.

Submitted: December 29, 2015
Accepted: May 28, 2016

Citation: Gao SS, Jia Y, Zhang M, et al. Optical coherence tomography angiography. *Invest Ophthalmol Vis Sci*. 2016;57:OCT27–OCT36. DOI:10.1167/iovs.15-19043

Optical coherence tomography angiography (OCTA) is a noninvasive approach that can visualize blood vessels down to the capillary level. With the advent of high-speed OCT and efficient algorithms, practical OCTA of ocular circulation is now available to ophthalmologists. Clinical investigations that used OCTA have increased exponentially in the past few years. This review will cover the history of OCTA and survey its most important clinical applications. The salient problems in the interpretation and analysis of OCTA are described, and recent advances are highlighted.

Keywords: optical coherence tomography, optical coherence tomography angiography, angiography, retina

Optical coherence tomography (OCT) is a noninvasive, depth-resolved imaging technique based on low-coherence interferometry. Optical coherence tomography generates structural images of anatomy based on back-reflected light. In the quarter-century since its inception,[1] OCT has seen rapid and wide adoption in ophthalmology. Improvements in sensitivity, acquisition speed, and resolution[2] have enabled volumetric imaging of ocular structures with micrometer-scale depth resolution. Although conventional structural OCT aids the clinician in visualizing the anatomic changes that impact vision, it offers poor contrast between small blood vessels and static tissue in most retinal layers. As a result, structural OCT is not used clinically to identify vascular changes such as capillary dropout or pathologic new vessel growth in AMD and diabetic retinopathy that can lead to vision loss.

To visualize vascular changes, the most commonly used angiographic techniques in clinical practice are fluorescein (FA) or indocyanine green angiography (ICGA). Fluorescein is typically used to visualize the retinal vasculature, while ICGA is used to see the choroidal vasculature. While useful, they require intravenous dye injection, which is time consuming and can have adverse side effects.[3,4] In addition, dye leakage and staining blur the boundaries of capillary dropout or neovascularization. Finally, these techniques provide little depth information due to the two-dimensional (2D) nature of the acquired images.

In order to develop a no-injection, dye-free method for visualizing ocular vasculature, a number of functional extensions of OCT has been explored. These techniques aim to contrast blood vessels from static tissue by assessing the change in the OCT signal caused by flowing blood cells. These intrinsic contrasts can be broadly classified as Doppler shift and speckle variance/decorrelation. This review will provide a historic overview of OCTA techniques based on these principles of flow detection. It will furthermore highlight the developments in post-processing and visualization tools that aid clinical interpretation. We want to emphasize that while Doppler OCT and certain implementations of OCTA both use phase information, the fundamental goals of Doppler OCT and OCTA are different. Doppler OCT uses the Doppler phase shift to quantify blood flow in larger vessels and measure total retinal blood flow,[5] an application that we will not review, while OCTA is more concerned about separating moving scatters from static background tissue to create angiograms.[6]

Label-Free Angiography

For more than half a century, scientists, engineers, and clinicians have collaborated to devise technologies to visualize and quantify changes in the retinal and choroidal vascular networks that supply the eye. Techniques such as ultrasound color Doppler imaging, laser Doppler velocimetry, laser speckle assessment, and blue field entopic technique have provided valuable insights into retinal physiology, but have not seen wide clinical use.[7] The limitations of these approaches include difficulty of use, poor reproducibility, large population variation in blood flow parameters, or limited availability of single-use instruments. Because OCT systems are widely used in ophthalmology, its application to blood flow visualization and measurement could make clinical use more practical. Since the early days of time-domain OCT, Doppler OCT has been explored as a tool for blood flow imaging. Doppler OCT uses the flow-induced Doppler phase shift between adjacent A-scans to calculate axial velocity.[8,9] Although Doppler OCT could measure and quantify blood velocity in larger vessels (Fig. 1A),[10] it is not well suited for angiography of retinal and choroidal microvasculature, where vessels are nearly perpendicular to the OCT beam.

Due to the slow speed of time-domain systems and the challenge posed by eye motion, volumetric angiography was not feasible until development of the two Fourier-domain OCT implementations[11–13]: spectral-domain (SD-OCT)[14,15] and swept-source.[16,17] When first introduced, Fourier-domain OCT already had a roughly 50-fold improvement in acquisition speed

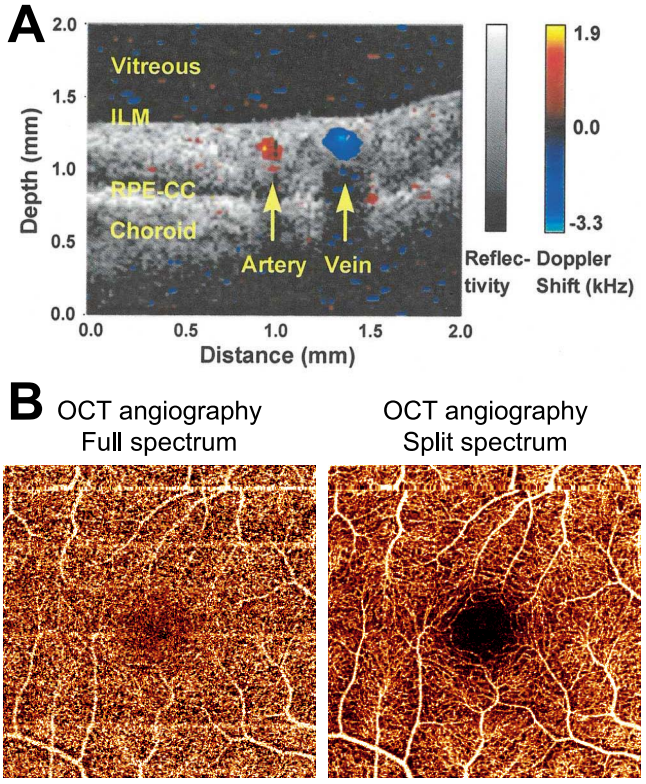

Figure 1. **(A)** The first demonstration of blood flow imaging in the living human eye with OCT. B-scan image of central vessels superior to the optic nerve head with Doppler shift signal (*false color*) overlaid on structural OCT (*gray scale*).[10] Reprinted with permission from Yazdanfar S, Rollins AM, Izatt JA. Imaging and velocimetry of the human retinal circulation with color Doppler optical coherence tomography. *Opt Lett*. 2000;25:1448–1450. © 2000 Optical Society of America. **(B)** Amplitude-decorrelation angiography of the macula (3 × 3–mm area) using full-spectrum (*left*) and split-spectrum processing (*right*). En face angiograms represent the maximum flow projection in the inner retina slab. Split-spectrum processing reduced noise and improved visualization of the retinal vascular network.

over time-domain OCT. In 2006, Makita et al.[18] used an 18.7-kHz SD-OCT system to perform volumetric angiography and visualization of retinal and choroidal vasculature. As noted by Makita et al.,[18] the standard deviation/variance[19] or power[20,21] of the Doppler signal provided better results than the Doppler shift. Another approach called optical microangiography (OMAG) incorporated the amplitude of the OCT signal in addition to phase. An et al.[22] suggested that OMAG was better able to identify the microvasculature than previous methods utilizing only phase information.

With the continued improvement of OCT system speeds due to hardware advances, methods for OCTA shifted from comparing between adjacent A-scans to between sequential cross-sectional B-scans. The increased time separation ensured that slower flow in the microvasculature would be detected. In 2009, Fingler et al.[23] used a 25-kHz SD-OCT system and a phase variance approach over 10 repeat B-scans at the same location to show microvasculature that was analogous to FA in human eyes. In 2011, Kim et al.[24] used a 125-kHz SD-OCT system to image with a larger field of view. They used montaging/stitching of 10 volumes to generate an OCT angiogram with coverage comparable to FA.

While phase-based approaches have been successful, they required precise removal of background phase noise due to bulk tissue motion or from system instabilities. Within an OCT system, phase noise can arise from scanning mirrors or a swept-source laser.[25,26] Although several methods exist to compensate for phase noise[20,27,28] and improve system phase stability,[29–32] an alternative is to use the variation in amplitude or intensity of the OCT signal to detect flow instead.

Optical coherence tomography angiography based on amplitude or intensity was initially described in 2005, when Barton et al.[33] adapted laser speckle analysis for time-domain OCT. Speckle arises as a property of the interferometric nature of OCT, and speckle variation contains information regarding the motion of scatterers.[34,35] Specifically, the speckle pattern stays relatively constant over time for static objects while the pattern changes for objects in motion. Mariampillai et al.[36] extended the technique and presented speckle variance detection of microvasculature in a dorsal skinfold model using a swept-source OCT system in 2008. In their work, speckle variance was calculated as the variance of the OCT reflectance amplitude over three repeated B-scans at the same location. In optimizing the method, Mariampillai et al.[37] noted in 2010 that the B-scan rates for repeat scans needed to be fast enough such that bulk motion between B-scans was less than the OCT beam waist radius.[37] Although "speckle variance" has been historically associated with amplitude-based OCTA, fundamentally both amplitude and phase-based flow detection are based on variation in the speckle pattern and therefore provide largely equivalent information.[38] In addition to speckle variance, another intensity-based OCTA approach was termed correlation mapping.[39] In correlation mapping OCTA, cross-correlation of a grid on adjacent B-scans was performed to identify vasculature (weak correlation) versus static tissue (strong correlation).

Optical coherence tomography angiography of retinal microvasculature in the human eye using methods based on amplitude or intensity was demonstrated in 2012. Motaghiannezem et al.[40] used logarithmic intensity variance and differential logarithmic intensity variance to capture the microvascular network near the fovea. In addition, Jia et al.[41] developed an efficient signal processing algorithm called split-spectrum amplitude-decorrelation angiography (SSADA). Split-spectrum amplitude-decorrelation angiography sacrificed axial resolution by splitting the OCT signal into different spectral bands to increase the number of usable image frames without increasing scanning time or decreasing scan density. When spectrally-split amplitude-decorrelation images were combined, the flow signal-to-noise ratio was increased (Fig. 1B). After optimization,[42] SSADA was able to produce angiograms of retinal and choroidal vasculature with only two consecutive B-scans.

As a quick summary of the different OCTA methods, we have simplified and classified the aforementioned as well as a few more recently developed methods in the Table. The methods are classified based on use of Doppler shift or speckle variance/decorrelation and whether they use full-spectrum or split-spectrum processing.

While each OCTA method can compensate for bulk tissue motion within a B-scan,[20,27,28,41] saccadic eye motion between B-scans could disrupt vessel continuity and reduce the quality of the final angiogram. Different approaches have been explored to address this issue. Because motion in two consecutive scans will be different, registering multiple scans is a potential solution. Orthogonal registration of one x-priority and one y-priority scan has been demonstrated to reduce motion artifacts.[47] Alternatively, incorporating eye tracking with the OCTA scan can minimize motion artifacts as well.[48]

Table. Simplified Summary of the Different Implementations of OCTA

		Speckle Variance or Decorrelation		
	Doppler Shift	**Amplitude or Intensity**	**Phase**	**Complex**
Full spectrum	Doppler[8–10]	Speckle variance[33]	Phase variance[19,23]	OMAG[43,44]
Split spectrum	Doppler[45,46]	SSADA[41,42]	SSPGA*	SSAPGA*

SSPGA, split-spectrum phase-gradient angiography; SSAPGA, split-spectrum amplitude and phase-gradient angiography.
* Liu G, Jia Y, Chandwani R, Pechauer AD, Huang D. Phase-gradient optical coherence tomography angiography. Denver, Colorado, May 2, 2015. ARVO Imaging in the Eye Conference.

Pathway to Clinical Usability

The interest in OCTA has grown dramatically in the past few years. This was aided by technology transfer of SSADA and an orthogonal registration approach[47] to Optovue, Inc., who then worked quickly to implement and make OCTA available as a research tool to the wider ophthalmic community on their commercial, SD-OCT platform. These events spurred Carl Zeiss Meditec, Inc. to adapt OMAG for their eye-tracking enabled SD-OCT system as well as other OCT companies to incorporate OCTA in their systems. Interpretation of OCTA, however, relies heavily on software to improve ease of use and facilitate analysis of collected data (Fig. 2). Methods and approaches to segment retinal layers for en face display and generate multicolor composite angiograms, which combine flow information from several en face slabs or combine flow and structural data will be reviewed.

En Face Visualization of Segmented Tissue Slabs

While OCT started as a predominantly cross-sectional imaging modality, OCTA was clinically used as an en face imaging modality from the start. This was enabled by initial work establishing the en face approach.[49–52] Optical coherence tomography angiography uses previously established techniques for automated segmentation of anatomic reference planes[53–55] such as the inner limiting membrane (ILM) and Bruch's membrane (BM). Appropriate tissue layers or "slabs" can then be defined based on these references planes. En face presentation of these slabs can produce angiograms similar to FA or ICGA.

Accurate segmentation is important for clinical interpretation. In diseased eyes, pathologies such as drusen, intraretinal cysts, edema, or subretinal fluid can make automated segmentation less robust. Although significant improvements have been made,[56–58] expert manual correction is sometimes necessary. Software that aids or reduces the workload required for manual correction of volumetric data is beneficial.[58,59]

Color Coding of Vessel or Slab Depth

Color coding is a common method used to convey additional information. In OCTA, color could be used to convey depth relative to a simple reference plane.[24] More often, color was used to represent flow in different segmented tissue slabs.[18,60] This allowed for clear visualization of retinal circulation in the inner retinal slab (between ILM and the outer boundary of the outer plexiform layer [OPL]) and choroidal circulation in the choroidal slab (below BM) on one angiogram. This division could be further refined, with retinal circulation divided between two or more plexuses and choroidal circulation divided into the choriocapillaris and deeper choroid. Abnormal vessels could also be visualized this way, with choroidal neovascularization (CNV; Fig. 2) seen in the outer retinal slab (between the outer boundary of OPL and BM) and retinal neovascularization in the vitreous slab (above ILM).[61,62] Furthermore, color coding can also be used to overlay flow information on structural OCT B-scans (Fig. 2).

Clinical Applications

In OCTA, diseases manifest as the abnormal presence of flow (neovascularization), anomalous vessel geometry (dilated vessels, aneurysms), or the absence of flow (nonperfusion/capillary dropout). These three types of abnormalities exist in almost all retinal and choroidal vascular diseases. Therefore, OCTA is widely applicable even though it cannot detect dye leakage or staining, which are the primary abnormalities detected by FA. In traditional dye-based angiography, retinal, choroidal, and abnormal circulations are all flattened into one 2D image. In contrast, OCTA data is three-dimensional (3D) and can be visualized in finely divided tissue slabs, which aid in the detection of pathologies.

Beginning in the vitreous, retinal neovascularization protruding above the ILM has been visualized in cases of diabetic retinopathy.[62,64,65] In the inner retina, retinal capillary dropout has been observed in diabetic retinopathy,[62,64–66] artery occlusion,[67,68] vein occlusion,[67,69,70] and glaucoma.[71] Enlarged foveal avascular zone has been described in diabetic retinopathy as well.[72–74] Additionally, observations regarding anomalous vascular formations such as macular telangiectasia[75–77] and microaneurysms in diabetic retinopathy[64,66] have been reported. Visualization of the deep retinal capillary plexus has provided new information regarding impaired flow in diseases such as retinal arterial occlusion[68] and paracentral acute middle maculopathy.[78] More posteriorly is the outer retina between the outer nuclear layer and BM This slab is used when assessing CNV.[61,65,79–84] Neovascularization has also been described in polypoidal choroidal vasculopathy,[85,86] pachychoroid neovasculopathy,[87] and central serous retinopathy.[88–90] Classification of CNV into type I, II, and/or III can be aided by use of composite structure and flow cross-sectional scans.[61]

Below BM at the choriocapillaris or choroid, capillary dropout has been assessed in choroideremia[65] and in areas of geographic atrophy in dry AMD.[65,91,92] In most cases of neovascularization, the abnormal vessels can be seen at these deeper layers as well due to the projection artifact. Therefore, CNV can also be visualized in the choroidal slabs.

Within the optic nerve head, perfusion has been investigated in cases of glaucoma[93] and multiple sclerosis.[94]

In summary, clinical investigations of OCTA have already demonstrated its potential in a wide variety of retinal and optic nerve diseases.

Artifacts

Although OCTA shows great promise, interpretation of OCTA must be done with knowledge of the possible image artifacts.[95–97] Motion error and improper software correction

Investigative Ophthalmology & Visual Science

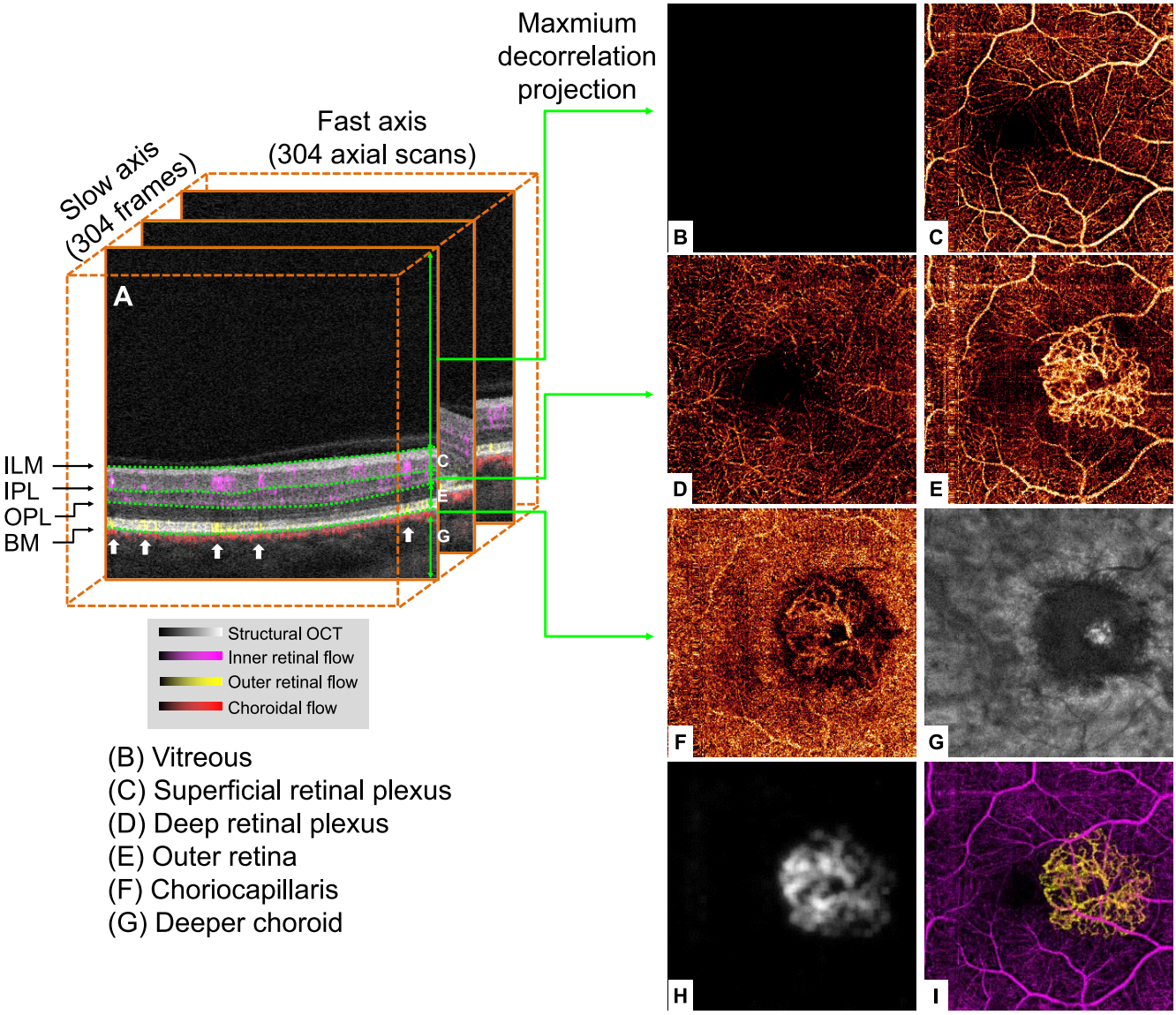

Figure 2. Segmentation and processing of OCTA. Optical coherence tomography angiography was performed on a 70-kHz SD-OCT with a center wavelength of 840 nm and axial resolution of 5 μm in tissue. (**A**) The volumetric OCTA scan comprised 304 cross-sectional frames along the slow scan axis. Flow in each frame was computed using the SSADA algorithm. The cross-sectional angiogram shows blood flow (*color*) overlaid on structural OCT (*gray scale*). It shows that flow in inner retinal vessels (*purple*) are projected onto the RPE complex (indicated by *white arrows*) – this is called "flow projection artifact." Image processing software separates the vitreous, inner retinal layers, outer retinal layer, and choroidal layers along the ILM and outer boundaries of the inner plexiform layer (IPL), OPL, and BM (*dotted green lines*). Maximum flow projection or mean reflectance projection was used to produce en face images. (**B**) The vitreous angiogram shows the absence of vascular flow. (**C**) The superficial inner retinal angiogram shows normal retinal circulation with a foveal avascular zone. Residual motion artifact in the form of a *horizontal line* is seen near the top of the angiogram. (**D**) The deep inner retina angiogram shows the deep retinal plexus. (**E**) The outer retina slab shows choroidal neovascularization (CNV) along with flow projection artifacts cast by the retinal circulation. (**F**) The choriocapillaris angiogram. (**G**) The deeper choroid en face structural OCT. (**H**) Detection of the CNV using a saliency-based approach.[63] (**I**) Composite en face angiogram of the inner retina (*purple*) and CNV (*yellow*).

can lead to vessel duplication, residual motion lines, and vessel discontinuity. Optical coherence tomography angiography also suffers from shadowgraphic flow projection artifacts (Fig. 2), which arise from fluctuating shadows cast by flowing blood that result in variation of the OCT signal in deeper layers. This is particularly apparent in angiograms of the outer retina. Inner retinal vessel projections on the highly reflective RPE in the outer retina produce false positive signal, which can interfere with CNV identification. Masking larger inner retinal vessels[61] or all inner retinal vessels[63,98] can help. The flow signal at areas with high or low OCT reflectance signal also need to be viewed with skepticism. Structures with high OCT reflectance such as hard exudate appear to amplify the signal from motion or projection artifact.[99] On the other hand, the lack of flow signal may be a result of shadowing and low OCT reflectance instead of true nonperfusion. Phantom studies looking at the relationship between flow and OCT signal amplitude may prove insightful.[100]

Quantification

Objective quantification of flow information is of great interest with regards to disease diagnosis and management. Two

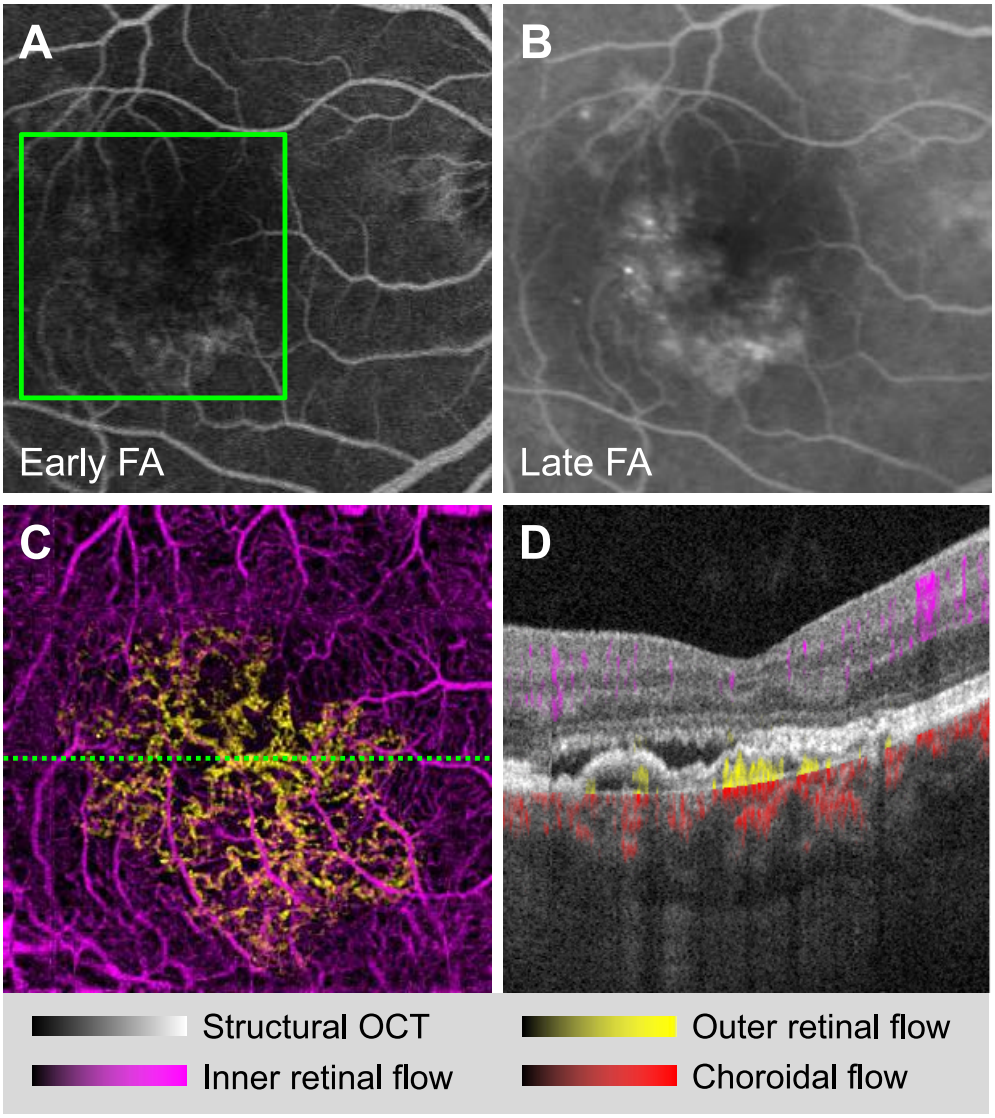

Figure 3. A case of central serous chorioretinopathy (CSCR). (**A**) Early-phase FA showing leakage. (**B**) Late-phase FA showing staining. However, FA could not determine whether the leakage was due to CSCR or secondary CNV. (**C**) A 3 × 3–mm en face spectral OCTA of the *boxed region* in *panel A*. (**D**) Cross-sectional OCTA corresponding to the *green line* in *panel C*. Optical coherence tomography angiography revealed flow beneath the RPE consistent with type 1 CNV. Optical coherence tomography angiography was useful in making the decision to treat this patient with anti-VEGF.

straightforward metrics that can be calculated from en face angiograms are flow index and vessel density.[93] Flow index is calculated as the average flow signal (which is correlated with flow velocity[101]) in a selected region, and vessel density is calculated as the percentage area occupied by vessels and microvasculature. Initial studies suggest that these metrics can have good repeatability and reproducibility.[71,102,103]

To more directly assess capillary dropout and neovascularization, however, additional metrics have been investigated. Capillary dropout or nonperfusion area refers to significant area (larger than the normal gap between capillaries) devoid of flow signal that would normally be vascular.[65] In the inner retina, detection of capillary dropout together with vessel density and/or flow index quantification has applications in diseases such as diabetic retinopathy,[65,103] glaucoma,[71] and optic neuritis.[94] In the choriocapillaris, assessing dropout would be important for AMD[65,91,92] and retinal degenerative diseases such as choroideremia.[65] Other approaches to assessing abnormal flow regions include characterization of the fractal dimension of vessel lines[104] and perfusion density mapping.[105]

Neovascularization area is the sum of pixel areas in a pathologic neovascular net identified on the en face OCT angiogram.[61] In proliferative diabetic retinopathy, the area is of neovascularization above the ILM or optic nerve head.[62,64] In neovascular AMD and other causes of CNV, the area of neovascularization is in the outer retina.[61,63] Other qualitative and quantitative metrics to describe the morphology of the CNV are also being explored.[81,82]

Quantitative metrics derived from OCTA have the potential to serve as new biomarkers of disease. However, well-designed validation studies and studies to determine repeatability and reproducibility are currently lacking. As OCTA research progresses, this will likely change. Although, validation studies may be difficult in cases where another noninvasive method is not available – for example, in the case of visualizing choriocapillaris.

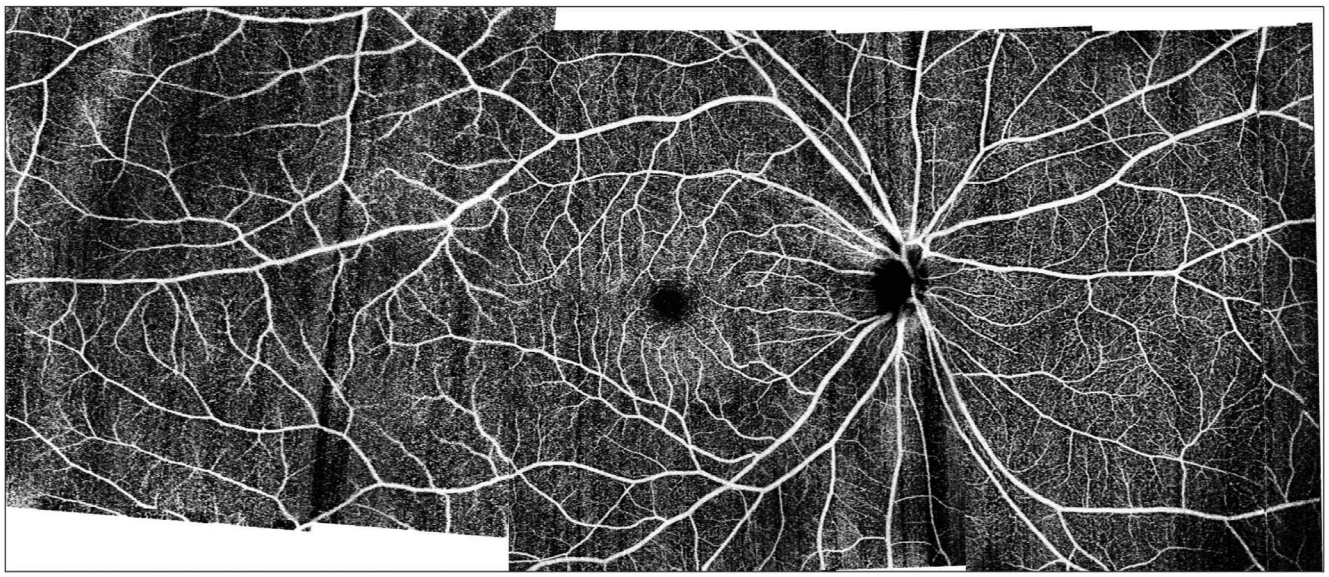

FIGURE 4. Ultra-widefield OCTA (~20-mm width, 10-mm height, 7-mm depth) of the retinal circulation generated by montaging four scans from a 200-kHz swept-source OCT system.

DISCUSSION AND FUTURE DIRECTIONS

Optical coherence tomography angiography is one of the most promising functional extensions of OCT. Despite its recent introduction, the potential clinical impact of OCTA can already be felt. A number of novel findings were made possible with OCTA. In AMD, OCTA could fully visualize CNV that are occult (poorly visualized) on FA. Interestingly, OCTA was able to identify a class of nonexudative CNV, which neither leak on FA nor exude retinal fluid on structural OCT.[92,106,107] The natural history and proper management of this new type of CNV is under investigation. Optical coherence tomography angiography is also able to visualize the closure of branch CNV vessels after anti-VEGF injection and their reopening/remodeling over time.[108,109] Rebound of CNV vessel area can precede fluid reaccumulation[83] and may be helpful for guiding the timing of therapy. In central serous chorioretinopathy, OCTA can more reliably determine the presence of CNV, which can be difficult to assess with FA (Fig. 3).[89] This is useful in identifying those who would benefit from anti-VEGF therapy. In diabetic retinopathy, OCTA can visualize small retinal neovascularizations into the vitreous which may be confused as microaneurysms on FA.[62] Optical coherence tomography angiography is uniquely capable of detecting capillary dropout in the different vascular plexuses in the inner retina, which may be useful in diagnostic or prognostic evaluation of diabetic retinopathy, vein/artery occlusion, and other ischemic diseases. Furthermore, the depth-resolved nature of OCTA improves visualization and localization of pathologic features. This has been particularly useful in diseases that were previously difficult to diagnose or classify using FA and ICGA. For example, in macular telangiectasia, retinal microvascular abnormalities and vascular anastomosis with subretinal neovascularization and choroidal circulation can now be visualized with OCTA.[77,110]

While OCTA has distinct advantages over FA and ICGA, it has its own set of limitations. Unlike FA, OCTA does not assess leakage. This is an advantage for OCTA during quantification as leakage can blur boundaries, but leakage gives additional information with regards to the integrity of the vasculature. Additionally, widefield FA is clinically available while widefield OCTA is limited to ultrahigh-speed laboratory prototypes at the moment. Going forward, we expect to see continued advances in hardware and software, which should expand the field of view of OCTA. Because at least two repeat scans are required for motion contrast, OCTA will inherently require more time than simple structural scans. As a result, current system speeds restrict the field of view or alternatively limit the transverse sampling density. Faster systems based on swept-source OCT technology coupled with improved eye tracking[48] or registration[48] is a potential solution. Montaging of multiple scans is also possible (Fig. 4).[24,111,112] As scans extend more peripherally, however, dynamic focusing[113] and increased imaging depth range[114] are needed to compensate for the increased curvature of the retina.

This interest in faster systems has led to discussions of the differences between SD-OCTA and swept-source OCTA. Direct comparisons are, however, difficult due to differences in the speed, which affects the sensitivity of flow detection, and operating wavelengths, which affects light scattering and penetration as well as resolution, of typical systems. While these differences can contribute to differences in the resulting OCTA angiograms, they are not inherent to the technologies themselves. The only intrinsic different between these two Fourier-domain OCT implementations is that SD-OCT is more susceptible to interferometric fringe washout artifact,[25] which is apparent only in large retinal vessels in the central optic nerve head.

The 3D nature of OCTA is both a blessing and a curse. The large 3D image cube needs to be segmented for detection and quantification of pathologies. And the clinician may need to scroll through many tissue layers to locate the pathology. Improvements in automated computer software for anatomic segmentation, pathology detection, and quantitation will make OCTA easier to use. In conjunction, there is a need for improved algorithms to reduce projection, shadow, and motion artifacts that often make OCTA difficult to interpret. This is an area of active research and rapid development. For example, advanced algorithms to remove shadowgraphic projection artifact[115] can already resolve three distinct retinal plexuses in the macula (Fig. 5).

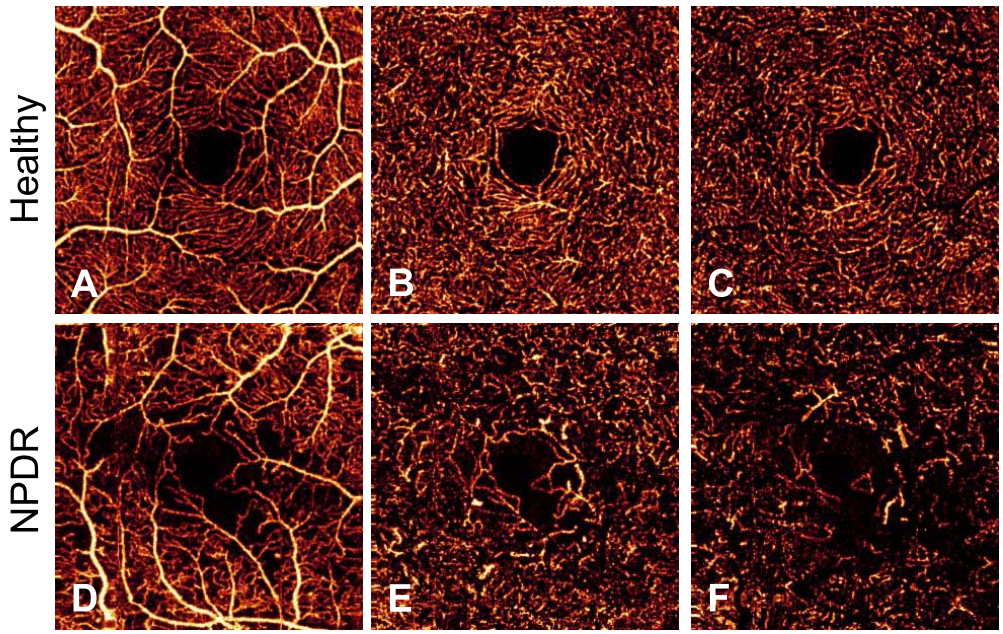

Figure 5. (*Top*) Projection-resolved OCTA[115] of a healthy eye shows three distinct plexuses: (**A**) superficial, in the nerve fiber and ganglion cell layers; (**B**) intermediate, between the inner plexiform and inner nuclear layers; and (**C**) deep, between the inner nuclear and outer plexiform layers. The plexuses merge at the edge of the foveal avascular zone. (*Bottom*) Optical coherence tomography angiography of an eye with nonproliferative diabetic retinopathy (NPDR) showing incongruent areas of capillary nonperfusion are present in the three plexuses. Dilated shunt vessels are seen in the intermediate (**E**) and deep (**F**) plexuses, in contrast with the uniform capillary network in the healthy eye. Reprinted with permission from Zhang M, Hwang TS, Campbell JP, et al. Projection-resolved optical coherence tomographic angiography. *Biomed Opt Express* 2016;7:816–828. © 2016 Optical Society of America.

Because OCTA is economical, noninvasive, and does not even require the use of bright visible light, it can be used more frequently than traditional angiography, which requires intravenous dye injection. Thus, we expect that OCTA could be used for high-volume applications such as the routine screening of diabetic retinopathy and regular follow-up of AMD. With the technological improvements that can be foreseen in the near future, we believe OCTA will become an important part of standard eye care.

Acknowledgments

Supported by National Institutes of Health (Bethesda, MD, USA) Grants R01EY024544, DP3DK104397, R01EY023285, P30EY010572, UL1TR000128, R01EY018184, and an unrestricted grant from Research to Prevent Blindness (New York, NY, USA).

Disclosure: **S.S. Gao**, None; **Y. Jia**, Optovue (F), P; **M. Zhang**, None; **J.P. Su**, None; **G. Liu**, None; **T.S. Hwang**, None; **S.T. Bailey**, None; **D. Huang**, Optovue (F, I, R), P

References

1. Huang D, Swanson EA, Lin CP, et al. Optical coherence tomography. *Science*. 1991;254:1178–1181.
2. Drexler W, Liu M, Kumar A, Kamali T, Unterhuber A, Leitgeb RA. Optical coherence tomography today: speed, contrast, and multimodality. *J Biomed Opt*. 2014;19:071412.
3. Hope-Ross M, Yannuzzi LA, Gragoudas ES, et al. Adverse reactions due to indocyanine green. *Ophthalmology*. 1994; 101:529–533.
4. Lopez-Saez MP, Ordoqui E, Tornero P, et al. Fluorescein-induced allergic reaction. *Ann Allergy Asthma Immunol*. 1998;81:428–430.
5. Leitgeb RA, Werkmeister RM, Blatter C, Schmetterer L. Doppler optical coherence tomography. *Prog Retin Eye Res*. 2014;41:26–43.
6. Wang RK, Jacques SL, Ma Z, Hurst S, Hanson SR, Gruber A. Three dimensional optical angiography. *Opt Express*. 2007; 15:4083–4097.
7. Schmetterer L, Garhofer G. How can blood flow be measured? *Surv Ophthalmol*. 2007;52(suppl 2):S134–S138.
8. Chen Z, Milner TE, Srinivas S, et al. Noninvasive imaging of in vivo blood flow velocity using optical Doppler tomography. *Opt Lett*. 1997;22:1119–1121.
9. Zhao Y, Chen Z, Saxer C, Xiang S, de Boer JF, Nelson JS. Phase-resolved optical coherence tomography and optical Doppler tomography for imaging blood flow in human skin with fast scanning speed and high velocity sensitivity. *Opt Lett*. 2000; 25:114–116.
10. Yazdanfar S, Rollins AM, Izatt JA. Imaging and velocimetry of the human retinal circulation with color Doppler optical coherence tomography. *Opt Lett*. 2000;25:1448–1450.
11. Leitgeb R, Hitzenberger C, Fercher A. Performance of Fourier domain vs. time domain optical coherence tomography. *Opt Express*. 2003;11:889–894.
12. Choma M, Sarunic M, Yang C, Izatt J. Sensitivity advantage of swept source and Fourier domain optical coherence tomography. *Opt Express*. 2003;11:2183–2189.
13. de Boer JF, Cense B, Park BH, Pierce MC, Tearney GJ, Bouma BE. Improved signal-to-noise ratio in spectral-domain compared with time-domain optical coherence tomography. *Opt Lett*. 2003;28:2067–2069.
14. Wojtkowski M, Leitgeb R, Kowalczyk A, Bajraszewski T, Fercher AF. In vivo human retinal imaging by Fourier domain optical coherence tomography. *J Biomed Opt*. 2002;7:457–463.
15. Nassif N, Cense B, Park B, et al. In vivo high-resolution video-rate spectral-domain optical coherence tomography of the human retina and optic nerve. *Opt Express*. 2004;12:367–376.

16. Yun S, Tearney G, de Boer J, Iftimia N, Bouma B. High-speed optical frequency-domain imaging. *Opt Express*. 2003;11: 2953–2963.
17. Lee EC, de Boer JF, Mujat M, Lim H, Yun SH. In vivo optical frequency domain imaging of human retina and choroid. *Opt Express*. 2006;14:4403–4411.
18. Makita S, Hong Y, Yamanari M, Yatagai T, Yasuno Y. Optical coherence angiography. *Opt Express*. 2006;14:7821–7840.
19. Zhao Y, Chen Z, Saxer C, et al. Doppler standard deviation imaging for clinical monitoring of in vivo human skin blood flow. *Opt Lett*. 2000;25:1358–1360.
20. Yang V, Gordon M, Qi B, et al. High speed, wide velocity dynamic range Doppler optical coherence tomography (Part I): system design, signal processing, and performance. *Opt Express*. 2003;11:794–809.
21. Park B, Pierce MC, Cense B, et al. Real-time fiber-based multi-functional spectral-domain optical coherence tomography at 1.3 microm. *Opt Express*. 2005;13:3931–3944.
22. An L, Wang RK. In vivo volumetric imaging of vascular perfusion within human retina and choroids with optical micro-angiography. *Opt Express*. 2008;16:11438–11452.
23. Fingler J, Zawadzki RJ, Werner JS, Schwartz D, Fraser SE. Volumetric microvascular imaging of human retina using optical coherence tomography with a novel motion contrast technique. *Opt Express*. 2009;17:22190–22200.
24. Kim DY, Fingler J, Werner JS, Schwartz DM, Fraser SE, Zawadzki RJ. In vivo volumetric imaging of human retinal circulation with phase-variance optical coherence tomography. *Biomed Opt Express*. 2011;2:1504–1513.
25. Hendargo HC, McNabb RP, Dhalla AH, Shepherd N, Izatt JA. Doppler velocity detection limitations in spectrometer-based versus swept-source optical coherence tomography. *Biomed Opt Express*. 2011;2:2175–2188.
26. Meng-Tsan T, Ting-Ta C, Hao-Li L, et al. Microvascular imaging using swept-source optical coherence tomography with single-channel acquisition. *Applied Physics Express*. 2011;4: 097001.
27. Yang VXD, Gordon ML, Mok A, et al. Improved phase-resolved optical Doppler tomography using the Kasai velocity estimator and histogram segmentation. *Optics Communications*. 2002;208:209–214.
28. White B, Pierce M, Nassif N, et al. In vivo dynamic human retinal blood flow imaging using ultra-high-speed spectral domain optical coherence tomography. *Opt Express*. 2003; 11:3490–3497.
29. Vakoc B, Yun S, de Boer J, Tearney G, Bouma B. Phase-resolved optical frequency domain imaging. *Opt Express*. 2005;13:5483–5493.
30. Zhang J, Chen Z. In vivo blood flow imaging by a swept laser source based Fourier domain optical Doppler tomography. *Opt Express*. 2005;13:7449–7457.
31. Hong YJ, Makita S, Jaillon F, et al. High-penetration swept source Doppler optical coherence angiography by fully numerical phase stabilization. *Opt Express*. 2012;20:2740–2760.
32. Liu G, Tan O, Gao SS, et al. Postprocessing algorithms to minimize fixed-pattern artifact and reduce trigger jitter in swept source optical coherence tomography. *Opt Express*. 2015;23:9824–9834.
33. Barton J, Stromski S. Flow measurement without phase information in optical coherence tomography images. *Opt Express*. 2005;13:5234–5239.
34. Aizu Y, Asakura T. Bio-speckle phenomena and their application to the evaluation of blood flow. *Optics & Laser Technology*. 1991;23:205–219.
35. Briers JD. Speckle fluctuations and biomedical optics: implications and applications. *OPTICE*. 1993;32:277–283.
36. Mariampillai A, Standish BA, Moriyama EH, et al. Speckle variance detection of microvasculature using swept-source optical coherence tomography. *Opt Lett*. 2008;33:1530–1532.
37. Mariampillai A, Leung MK, Jarvi M, et al. Optimized speckle variance OCT imaging of microvasculature. *Opt Lett*. 2010; 35:1257–1259.
38. Liu G, Lin AJ, Tromberg BJ, Chen Z. A comparison of Doppler optical coherence tomography methods. *Biomed Opt Express*. 2012;3:2669–2680.
39. Enfield J, Jonathan E, Leahy M. In vivo imaging of the microcirculation of the volar forearm using correlation mapping optical coherence tomography (cmOCT). *Biomed Opt Express*. 2011;2:1184–1193.
40. Motaghiannezam R, Fraser S. Logarithmic intensity and speckle-based motion contrast methods for human retinal vasculature visualization using swept source optical coherence tomography. *Biomed Opt Express*. 2012;3:503–521.
41. Jia Y, Tan O, Tokayer J, et al. Split-spectrum amplitude-decorrelation angiography with optical coherence tomography. *Opt Express*. 2012;20:4710–4725.
42. Gao SS, Liu G, Huang D, Jia Y. Optimization of the split-spectrum amplitude-decorrelation angiography algorithm on a spectral optical coherence tomography system. *Opt Lett*. 2015;40:2305–2308.
43. Wang RK, An L, Francis P, Wilson DJ. Depth-resolved imaging of capillary networks in retina and choroid using ultrahigh sensitive optical microangiography. *Opt Lett*. 2010;35:1467–1469.
44. An L, Shen TT, Wang RK. Using ultrahigh sensitive optical microangiography to achieve comprehensive depth resolved microvasculature mapping for human retina. *J Biomed Opt*. 2011;16:106013.
45. Vuong B, Lee AM, Luk TW, et al. High speed, wide velocity dynamic range Doppler optical coherence tomography (Part IV): split spectrum processing in rotary catheter probes. *Opt Express*. 2014;22:7399–7415.
46. Tan O, Liu G, Liang L, et al. En face Doppler total retinal blood flow measurement with 70 kHz spectral optical coherence tomography. *J Biomed Opt*. 2015;20:066004.
47. Kraus MF, Liu JJ, Schottenhamml J, et al. Quantitative 3D-OCT motion correction with tilt and illumination correction, robust similarity measure and regularization. *Biomed Opt Express*. 2014;5:2591–2613.
48. Zhang Q, Huang Y, Zhang T, et al. Wide-field imaging of retinal vasculature using optical coherence tomography-based microangiography provided by motion tracking. *J Biomed Opt*. 2015;20:066008.
49. Podoleanu AG, Dobre GM, Jackson DA. En-face coherence imaging using galvanometer scanner modulation. *Opt Lett*. 1998;23:147–149.
50. Rogers J, Podoleanu A, Dobre G, Jackson D, Fitzke F. Topography and volume measurements of the optic nerve using en-face optical coherence tomography. *Opt Express*. 2001;9:533–545.
51. van Velthoven ME, Verbraak FD, Yannuzzi LA, Rosen RB, Podoleanu AG, de Smet MD. Imaging the retina by en face optical coherence tomography. *Retina*. 2006;26:129–136.
52. Gorczynska I, Srinivasan VJ, Vuong LN, et al. Projection OCT fundus imaging for visualising outer retinal pathology in non-exudative age-related macular degeneration. *Br J Ophthalmol*. 2009;93:603–609.
53. Ishikawa H, Stein DM, Wollstein G, Beaton S, Fujimoto JG, Schuman JS. Macular segmentation with optical coherence tomography. *Invest Ophthalmol Vis Sci*. 2005;46:2012–2017.
54. Tan O, Li G, Lu AT, Varma R, Huang D. Mapping of macular substructures with optical coherence tomography for glaucoma diagnosis. *Ophthalmology*. 2008;115:949–956.

55. Chiu SJ, Li XT, Nicholas P, Toth CA, Izatt JA, Farsiu S. Automatic segmentation of seven retinal layers in SDOCT images congruent with expert manual segmentation. *Opt Express*. 2010;18:19413–19428.
56. Chiu SJ, Izatt JA, O'Connell RV, Winter KP, Toth CA, Farsiu S. Validated automatic segmentation of AMD pathology including drusen and geographic atrophy in SD-OCT images. *Invest Ophthalmol Vis Sci*. 2012;53:53–61.
57. Chiu SJ, Allingham MJ, Mettu PS, Cousins SW, Izatt JA, Farsiu S. Kernel regression based segmentation of optical coherence tomography images with diabetic macular edema. *Biomed Opt Express*. 2015;6:1172–1194.
58. Zhang M, Wang J, Pechauer AD, et al. Advanced image processing for optical coherence tomographic angiography of macular diseases. *Biomed Opt Express*. 2015;6:4661–4675.
59. Yin X, Chao JR, Wang RK. User-guided segmentation for volumetric retinal optical coherence tomography images. *J Biomed Opt*. 2014;19:086020.
60. Miura M, Makita S, Iwasaki T, Yasuno Y. Three-dimensional visualization of ocular vascular pathology by optical coherence angiography in vivo. *Invest Ophthalmol Vis Sci*. 2011; 52:2689–2695.
61. Jia Y, Bailey ST, Wilson DJ, et al. Quantitative optical coherence tomography angiography of choroidal neovascularization in age-related macular degeneration. *Ophthalmology*. 2014;121:1435–1444.
62. Hwang TS, Jia Y, Gao SS, et al. Optical coherence tomography angiography features of diabetic retinopathy. *Retina*. 2015; 35:2371–2376.
63. Liu L, Gao SS, Bailey ST, Huang D, Li D, Jia Y. Automated choroidal neovascularization detection algorithm for optical coherence tomography angiography. *Biomed Opt Express*. 2015;6:3564–3576.
64. Ishibazawa A, Nagaoka T, Takahashi A, et al. Optical coherence tomography angiography in diabetic retinopathy: a prospective pilot study. *Am J Ophthalmol*. 2015;160:35–44.
65. Jia Y, Bailey ST, Hwang TS, et al. Quantitative optical coherence tomography angiography of vascular abnormalities in the living human eye. *Proc Natl Acad Sci U S A*. 2015; 112:E2395–E2402.
66. Couturier A, Mane V, Bonnin S, et al. Capillary plexus anomalies in diabetic retinopathy on optical coherence tomography angiography. *Retina*. 2015;35:2384–2391.
67. Mastropasqua R, Di Antonio L, Di Staso S, et al. Optical coherence tomography angiography in retinal vascular diseases and choroidal neovascularization. *J Ophthalmol*. 2015;2015:343515.
68. Bonini Filho MA, Adhi M, de Carlo TE, et al. Optical coherence tomography angiography in retinal artery occlusion. *Retina*. 2015;35:2339–2346.
69. Rispoli M, Savastano MC, Lumbroso B. Capillary network anomalies in branch retinal vein occlusion on optical coherence tomography angiography. *Retina*. 2015;35:2332–2338.
70. Nobre Cardoso J, PA, Keane, Sim DA, et al. Systematic evaluation of optical coherence tomography angiography in retinal vein occlusion. *Am J Ophthalmol*. 2016;163:93–107.
71. Liu L, Jia Y, Takusagawa HL, et al. Optical coherence tomography angiography of the peripapillary retina in glaucoma. *JAMA Ophthalmol*. 2015;133:1045–1052.
72. Kim DY, Fingler J, Zawadzki RJ, et al. Noninvasive imaging of the foveal avascular zone with high-speed, phase-variance optical coherence tomography. *Invest Ophthalmol Vis Sci*. 2012;53:85–92.
73. Freiberg FJ, Pfau M, Wons J, Wirth MA, Becker MD, Michels S. Optical coherence tomography angiography of the foveal avascular zone in diabetic retinopathy. *Graefes Arch Clin Exp Ophthalmol*. 2016;254:1051–1058.
74. Takase N, Nozaki M, Kato A, Ozeki H, Yoshida M, Ogura Y. Enlargement of foveal avascular zone in diabetic eyes evaluated by en face optical coherence tomography angiography. *Retina*. 2015;35:2377–2383.
75. Zeimer M, Gutfleisch M, Heimes B, Spital G, Lommatzsch A, Pauleikhoff D. Association between changes in macular vasculature in optical coherence tomography- and fluorescein- angiography and distribution of macular pigment in type 2 idiopathic macular telangiectasia. *Retina*. 2015;35:2307–2316.
76. Gaudric A, Krivosic V, Tadayoni R. Outer retina capillary invasion and ellipsoid zone loss in macular telangiectasia type 2 imaged by optical coherence tomography angiography. *Retina*. 2015;35:2300–2306.
77. Spaide RF, Klancnik JM Jr, Cooney MJ, et al. Volume-rendering optical coherence tomography angiography of macular telangiectasia type 2. *Ophthalmology*. 2015;122:2261–2269.
78. Sridhar J, Shahlaee A, Rahimy E, et al. Optical coherence tomography angiography and en face optical coherence tomography features of paracentral acute middle maculopathy. *Am J Ophthalmol*. 2015;160:1259–1268. e1252.
79. Moult E, Choi W, Waheed NK, et al. Ultrahigh-speed swept-source OCT angiography in exudative AMD. *Ophthalmic Surg Lasers Imaging Retina*. 2014;45:496–505.
80. Kuehlewein L, Bansal M, Lenis TL, et al. Optical coherence tomography angiography of type 1 neovascularization in age-related macular degeneration. *Am J Ophthalmol*. 2015;160: 739–748.e2.
81. de Carlo TE, Bonini Filho MA, Chin AT, et al. Spectral-domain optical coherence tomography angiography of choroidal neovascularization. *Ophthalmology*. 2015;122:1228–1238.
82. Coscas G, Lupidi M, Coscas F, Francais C, Cagini C, Souied EH. Optical coherence tomography angiography during follow-up: qualitative and quantitative analysis of mixed type I and II choroidal neovascularization after vascular endothelial growth factor trap therapy. *Ophthalmic Res*. 2015;54:57–63.
83. Huang D, Jia Y, Rispoli M, Tan O, Lumbroso B. Optical coherence tomography angiography of time course of choroidal neovascularization in response to anti-angiogenic treatment. *Retina*. 2015;35:2260–2264.
84. Kuehlewein L, Dansingani KK, de Carlo TE, et al. Optical coherence tomography angiography of type 3 neovascularization secondary to age-related macular degeneration. *Retina*. 2015;35:2229–2235.
85. Kim JY, Kwon OW, Oh HS, Kim SH, You YS. Optical coherence tomography angiography in patients with polypoidal choroidal vasculopathy [published online ahead of print November 30, 2015]. *Graefes Arch Clin Exp Ophthalmol*. doi:10.1097/IAE.0000000000000777.
86. Inoue M, Balaratnasingam C, Freund KB. Optical coherence tomography angiography of polypoidal choroidal vasculopathy and polypoidal choroidal neovascularization. *Retina*. 2015;35:2265–2274.
87. Dansingani KK, Balaratnasingam C, Klufas MA, Sarraf D, Freund KB. Optical coherence tomography angiography of shallow irregular pigment epithelial detachments in pachychoroid spectrum disease. *Am J Ophthalmol*. 2015;160:1243–1254.
88. Bonini Filho MA, de Carlo TE, Ferrara D. et al. Association of choroidal neovascularization and central serous chorioretinopathy with optical coherence tomography angiography. *JAMA Ophthalmol*. 2015;133:899–906.
89. McClintic SM, Jia Y, Huang D, Bailey ST. Optical coherence tomographic angiography of choroidal neovascularization

associated with central serous chorioretinopathy. *JAMA Ophthalmol*. 2015;133:1212–1214.

90. Costanzo E, Cohen SY, Miere A, et al. Optical coherence tomography angiography in central serous chorioretinopathy. *J Ophthalmol*. 2015;2015:134783.
91. Kim DY, Fingler J, Zawadzki RJ, et al. Optical imaging of the chorioretinal vasculature in the living human eye. *Proc Natl Acad Sci U S A*. 2013;110:14354–14359.
92. Choi W, Moult EM, Waheed NK, et al. Ultrahigh-speed, swept-source optical coherence tomography angiography in non-exudative age-related macular degeneration with geographic atrophy. *Ophthalmology*. 2015;122:2532–2544.
93. Jia Y, Morrison JC, Tokayer J, et al. Quantitative OCT angiography of optic nerve head blood flow. *Biomed Opt Express*. 2012;3:3127–3137.
94. Wang X, Jia Y, Spain R, et al. Optical coherence tomography angiography of optic nerve head and parafovea in multiple sclerosis. *Br J Ophthalmol*. 2014;98:1368–1373.
95. Spaide RF, Fujimoto JG, Waheed NK. Image artifacts in optical coherence tomography angiography. *Retina*. 2015;35:2163–2180.
96. Chen FK, Viljoen RD, Bukowska DM. Classification of image artefacts in optical coherence tomography angiography of the choroid in macular diseases [published online ahead of print November 19, 2015]. *Clin Experiment Ophthalmol*. doi: 10.1111/ceo.12683.
97. de Carlo TE, Romano A, Waheed NK, Duker JS. A review of optical coherence tomography angiography (OCTA). *International Journal of Retina and Vitreous*. 2015;1:1–15.
98. Zhang A, Zhang Q, Wang RK. Minimizing projection artifacts for accurate presentation of choroidal neovascularization in OCT micro-angiography. *Biomed Opt Express*. 2015;6:4130–4143.
99. Huang Y, Zhang Q, Wang RK. Efficient method to suppress artifacts caused by tissue hyper-reflections in optical microangiography of retina in vivo. *Biomed Opt Express*. 2015;6:1195–1208.
100. Zhang A, Wang RK. Feature space optical coherence tomography based micro-angiography. *Biomed Opt Express*. 2015;6:1919–1928.
101. Tokayer J, Jia Y, Dhalla AH, Huang D. Blood flow velocity quantification using split-spectrum amplitude-decorrelation angiography with optical coherence tomography. *Biomed Opt Express*. 2013;4:1909–1924.
102. Jia Y, Wei E, Wang X, et al. Optical coherence tomography angiography of optic disc perfusion in glaucoma. *Ophthalmology*. 2014;121:1322–1332.
103. Hwang TS, Gao SS, Liu L, et al. Automated quantification of capillary nonperfusion using optical coherence tomography angiography in diabetic retinopathy. *JAMA Ophthalmol*. 2016;1–7.
104. Schmoll T, Singh AS, Blatter C, et al. Imaging of the parafoveal capillary network and its integrity analysis using fractal dimension. *Biomed Opt Express*. 2011;2:1159–1168.
105. Agemy SA, Scripsema NK, Shah CM, et al. Retinal vascular perfusion density mapping using optical coherence tomography angiography in normals and diabetic retinopathy patients. *Retina*. 2015;35:2353–2363.
106. Palejwala NV, Jia Y, Gao SS, et al. Detection of nonexudative choroidal neovascularization in age-related macular degeneration with optical coherence tomography angiography. *Retina*. 2015;35:2204–2211.
107. Roisman L, Zhang Q, Wang RK, et al. Optical coherence tomography angiography of asymptomatic neovascularization in intermediate age-related macular degeneration. *Ophthalmology*. 2016;123:1309–1319.
108. Lumbroso B, Rispoli M, Savastano MC. Longitudinal optical coherence tomography-angiography study of type 2 naive choroidal neovascularization early response after treatment. *Retina*. 2015;35:2242–2251.
109. Spaide RF. Optical coherence tomography angiography signs of vascular abnormalization with antiangiogenic therapy for choroidal neovascularization. *Am J Ophthalmol*. 2015;160:6–16.
110. Zhang Q, Wang RK, Chen CL, et al. Swept source optical coherence tomography angiography of neovascular macular telangiectasia type 2. *Retina*. 2015;35:2285–2299.
111. Choi W, Mohler KJ, Potsaid B, et al. Choriocapillaris and choroidal microvasculature imaging with ultrahigh speed OCT angiography. *PLoS One*. 2013;8:e81499.
112. Hendargo HC, Estrada R, Chiu SJ, Tomasi C, Farsiu S, Izatt JA. Automated non-rigid registration and mosaicing for robust imaging of distinct retinal capillary beds using speckle variance optical coherence tomography. *Biomed Opt Express*. 2013;4:803–821.
113. Su JP, Li Y, Tang M, et al. Imaging the anterior eye with dynamic-focus swept-source optical coherence tomography. *J Biomed Opt*. 2015;20:126002.
114. Grulkowski I, Liu JJ, Potsaid B, et al. High-precision, high-accuracy ultralong-range swept-source optical coherence tomography using vertical cavity surface emitting laser light source. *Opt Lett*. 2013;38:673–675.
115. Zhang M, Hwang TS, Campbell JP, et al. Projection-resolved optical coherence tomographic angiography. *Biomed Opt Express*. 2016;7:816–828.

Investigative Ophthalmology & Visual Science